Enabling Distributed Low Radio Frequency Arrays - Results of an Analog Campaign on Mt. Etna

Emanuel Staudinger, Robert Pöhlmann,
Siwei Zhang, and Armin Dammann
German Aerospace Center (DLR)
Institute of Communications and Navigation
Münchener Str. 20
82234 Wessling, Germany
Emanuel.Staudinger@DLR.de

Riccardo Giubilato, Ryo Sakagami, Peter Lehner,
Martin J. Schuster, Andreas Dömel, Bernhard Vodermayer,
Andre F. Prince, and Armin Wedler
German Aerospace Center (DLR)
Institute of Robotics and Mechatronics
Münchener Str. 20
82234 Wessling, Germany

Abstract—**Measurement of the red-shifted 21-cm signal of neutral hydrogen, and thus observing The Dark Ages is expected to be the holy grail of 21-cm Cosmology. A Radio-telescope to observe low radio frequency signals is needed, but radio interference on Earth and Earth's ionosphere blocking these signals are limiting science investigations in this field. Hence, such a radio-telescope composed of dozens to hundreds of antennas shall be deployed on the lunar far side. Such arrays are shielded from interference from Earth and Earth's ionosphere blocking very low radio frequencies is not present.**

Within the Helmholtz Future Topic Project Autonomous Robotic Networks to Help Modern Societies (ARCHES) we developed necessary technologies for autonomous robotic deployment of antenna elements, modular payload box design, and robust radio-localization to enable such distributed low-frequency arrays. In particular the antennas' positions must be determined accurately, such that the array can be operated as phased array. Our developments lead to the execution of an analog-demonstration on the volcano Mt. Etna, Sicily, Italy, in June and July 2022 over the course of four weeks. We successfully demonstrated the autonomous robotic deployment of antenna elements and our decentralized real-time radio-localization system to obtain the antenna element positions. Additionally, we showed a proof-of-concept operation of the phased array comprising four antenna elements: estimating the signal direction of arrival of a radio-beacon with unknown position, and the beamforming capabilities itself, for a carrier frequency of 20 MHz.

In this paper, we give insights into our developed technologies and the analog-demonstration on the volcano Mt. Etna, Sicily, Italy. We show results of the successfully executed mission and give an outlook how our developed technologies can be further used for lunar exploration.

TABLE OF CONTENTS

1. INTRODUCTION

The lunar far side has been identified as an ideal place for radio science and the deployment of radio telescopes [1], [2], [3]. In particular, the measurement of the red-shifted 21-cm signal of neutral hydrogen and thus, observing the so-called Dark Ages of the Universe is expected to be the holy grail of 21-cm Cosmology [2]. Such radio telescopes shall receive radio signals in a frequency range from few Megahertz to a couple of dozens Megahertz. Although such radio telescopes have been installed on Earth, such as the LOw-Frequency ARray [4], radio science is limited. Strong back-ground interference at low radio frequencies limit sensitivity and Earth's atmosphere blocks radio signals below 10 MHz, to name some limitations. Various concepts for radio telescopes on the lunar far side have been proposed, e.g., tethered arrays [5], or exploiting craters as a whole to form a telescope [6]. In general, low radio frequency arrays for the lunar far side will comprise dozens to hundreds of antenna elements spread in an area with edge lengths ranging from several hundred meters to kilometers (except lunar crater telescopes) [1]. A multitude of technologies is required to enable such arrays covering landers, robotic capabilities for deployment, accurate localization of antenna elements, and the antenna elements including array processing. To the best of our knowledge, the complete autonomous robotic deployment, localization of antenna elements, and a proof-of-concept array operation has not been demonstrated so far. In our work, we particularly focused on distributed (untethered) low radio frequency arrays, the technologies to enable them, and the demonstration in an analog environment.

The paper is organized as follows: Sec. 2 provides an overview of our analog campaign and the required technologies. In Sec. 3, we describe our modular payload carrier approach and the developed payload boxes. Details and results of the autonomous robotic array deployment, and a novel radio-localization system are provided in Sec. 4 and Sec. 5. The proof of concept array operation is described in Sec. 6. Finally, we discuss how our developed technologies can be used beyond the use-case of low radio frequency arrays in Sec. 7 and we summarize in Sec. 8.

2. THE ARCHES LOFAR MISSION

The aim of the Helmholtz Future Topic Project Autonomous Robotic Networks to Help Modern Societies (ARCHES) is to establish and strengthen cooperation in the field of robotics across the deep-sea domain and space domain among the German Helmholtz research centers [7]. The technological goal of the project is the development and demonstration of heterogeneous, autonomous, and networked robotic systems.

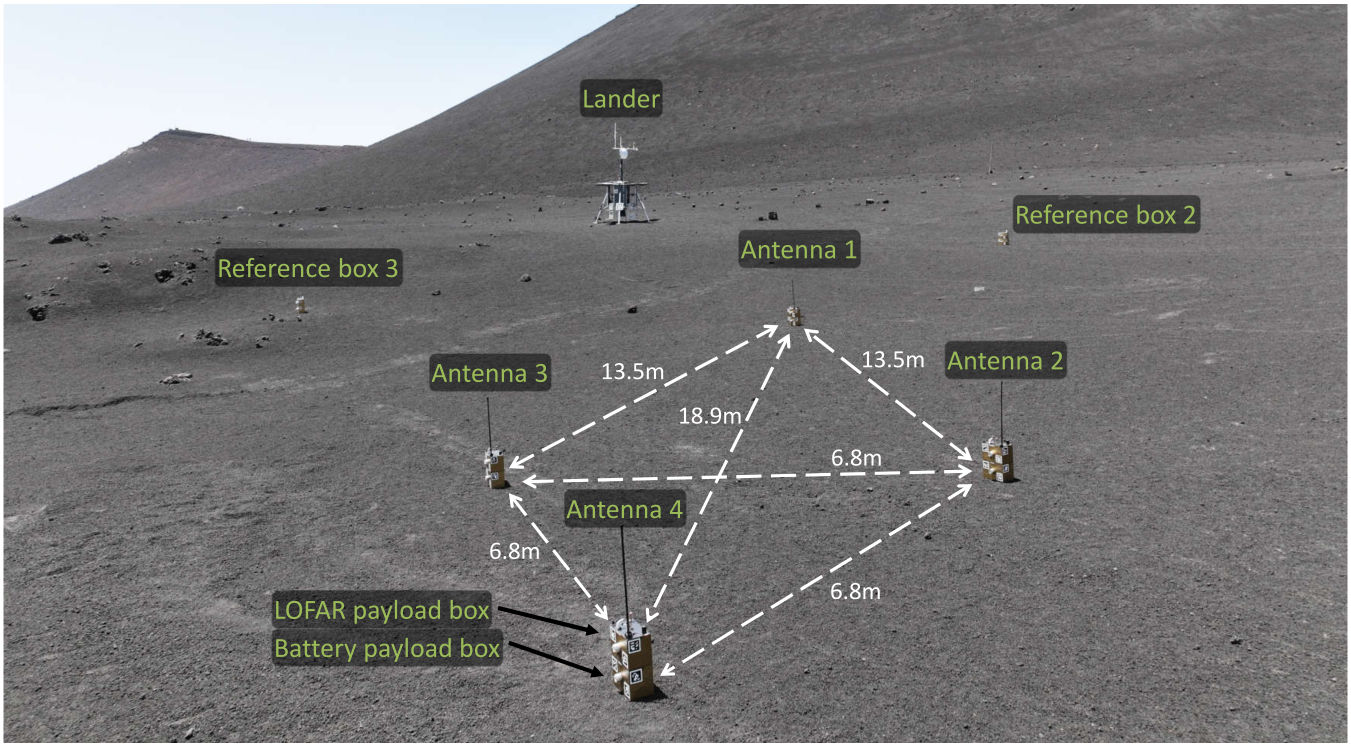

Figure 1: Experiment area on Mt. Etna, Sicily, Italy in June 2022 with four antenna elements placed in the field. Each antenna element consists of a battery payload box, and the ARCHES LOFAR payload box stacked on it.

In the space domain, three scientifically relevant use cases, referred to as ARCHES missions, have been identified: two in the geological exploration context, and one in the field of radio-astronomy. The latter has been termed ARCHES low frequency array (LOFAR) mission and is the core of this paper.

The goal of this mission was the demonstration of technologies for a distributed, non-tethered low radio frequency array in an analog environment comprising four antenna elements forming a phased array. Our technologies can be grouped as follows:

- Modular payload carriers, which include a battery payload box and the LOFAR payload box. The payload boxes are based on a modular approach and can be transported and manipulated by a small planetary exploration rover, our in-house developed Lightweight Rover Unit (LRU) [8].
- Autonomous robotic array deployment including the LRU design, autonomous vision-based navigation and multi-robot mapping, and payload box manipulation.
- Radio-localization system enabling accurate relative array localization once deployed in the field.
- Low radio frequency array processing and proof of concept array operation, including signal direction of arrival estimation and beamforming for a carrier frequency of $20\,\mathrm{MHz}$.

For analog demonstration, we chose an experiment area on Mt. Etna, Sicily, Italy, see Fig. 1. Over the course of four weeks in June and July 2022, we conducted pretests of individual components, and executed the mission. A general overview of the infrastructure setup is available in [7]. In this mission, the LRU2 picks a battery payload box from the lander and places it at a predefined location. It drives back to the lander, picks a LOFAR payload box, drives to the placed battery payload box, and stacks it. The picking process and navigation through the yet unexplored terrain is executed autonomously and a second rover named LRU1 without manipulation capabilities cooperatively supports the mapping and navigation process. Once the four antenna elements are deployed, all rovers leave the experiment area, and the spring antennas are released. Our radio-localization system is switched on to obtain the final geometry of the array accurately. The determined antenna positions are then used for the low radio frequency array operation: we determine the signal direction of arrival from a $20\,\mathrm{MHz}$ transmitter of unknown location placed in the field, and show the beamforming of the array.

In addition to the technological aspects of this mission, we included operational aspects as well. The overall mission has been executed from a main control room located in the city of Catania. This main control room was connected with the lander in the experiment site via a two-hop $20\,\mathrm{km}$ directional radio link. As a consequence, the operators in the main control room had to cope with limited signal bandwidth and latency. In the subsequent sections, we will describe our technologies in more detail and jointly present results from this mission.

3. MODULAR PAYLOAD CARRIERS

Modular Approach

We have developed the modular approach [9] of our robotic assets motivated by the complexity, heavy weight, and high costs of the rover systems utilized in current planetary exploration missions. With all their scientific components embedded in their bodies, these rovers lack the possibility to have parts replaced in case of permanent failure, which certainly increases the risk of the mission. Therefore, we

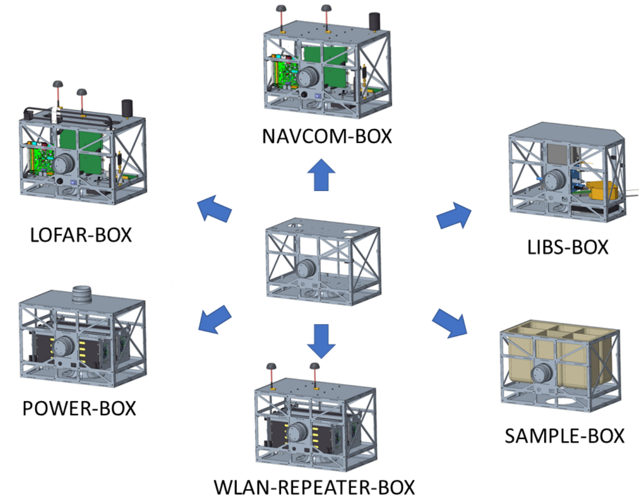

Figure 2: Family of payload boxes for ARCHES demonstration mission.

have introduced this new concept of lightweight universal rovers designed for planetary exploration equipped with a robotic manipulator and a standardized docking interface. The docking interface can connect to a set of tools and payload systems, which increase the versatility of the rover. This cost-effective and low-risk strategy was presented for the first time during the ROBEX project [10]. The LRU rover by the German Aerospace Center (DLR), provided with a Jaco manipulator arm and a DLR ENVICON docking interface was used to autonomously manipulate payload boxes with integrated seismometers. This was the origin of the modular standardized payload systems concept, which was further developed during the ARCHES project with a wider set of different payload modules. In Fig. 2, we can see the overview of the family of payload boxes. The implemented systems range from fully passive sample containers to highly integrated laser spectroscopy sensors and the LOFAR payload box presented in this paper. In addition, for ARCHES we have optimized the original payload system with the introduction of enhanced electromechanical interfaces and a standardized electronics infrastructure to support the system functionality [11].

All active payload boxes such as the LOFAR payload box contain a payload box infrastructure management system (PBIMS), which has a compact and flexible design. As shown in Fig. 3, the PBIMS provides power to the entire payload system with regulated power for up to seven different voltages. It also manages up to three different non-regulated input power sources to be fed to the main system voltage bus ranging from 24 V to 30 V. Furthermore, it includes onboard sensors, such as inertial measurement unit (IMU) and environmental sensors. It also has a broad spectrum of wired and wireless communication interfaces to provide telemetry data and power bus control to the field infrastructure or the computers within the payload box. The house-keeping system of the LOFAR payload box can interact directly with the PBIMS via an USB-based protocol and readout all corresponding bus voltages and bus currents of each subsystem. Thus, power saving strategies can be implemented to increase the power endurance of the LOFAR payload box and prolong the mission.

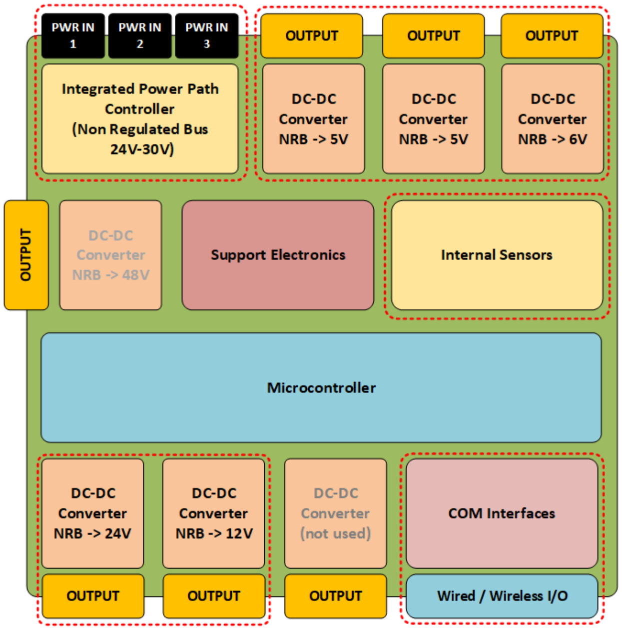

Figure 3: Payload box infrastructure management system diagram.

Power Payload Box

The power payload box has been designed to extend the power autonomy of several payload modules, such as the LOFAR payload box, which can be stacked on top of it. Its battery capacity of 400 Wh guarantees up to eight extra hours for a 50 W nominal consumption. This represents a complete day of operations in the field. The box includes two battery packs with a local battery management system (BMS), a PBIMS board to manage the power distribution and communication, and a set of electromechanical interfaces to allow the connection between the power supply box and external consumers. During the ARCHES demonstration mission, we used seven power payload boxes which provided additional power to four LOFAR payload boxes and three reference boxes. In our mission scenario, the internal battery packs can be hot-swapped by a person in the field. For a real lunar scenario, one would integrate foldable solar panels to allow for recharging and continuous operations.

LOFAR Payload Box

The LOFAR payload box is based on the modular approach and tailored to the analog campaign. A mandatory requirement from the robotics side has been the manipulation capability of the robotic arm, which limits the maximum weight of the box to 2.8 kg. All hardware components within the box are common off-the-shelf products. We had to balance weight, operational lifetime with the internal battery, and functionality. Fig. 4 shows the mechanical concept with its major components, which we will shortly describe next.

For communications to the lander, we use a wireless modem operating at 5.3 GHz. A ublox global navigation satellite system (GNSS) receiver, and a Raspberry PI as housekeeping computer provide ground-truth positional information. We use GNSS real-time kinematic (RTK) with a locally operated base station to obtain centimeter-accurate ground-truth. The radio-localization system consists of an Intel next unit of computing (NUC) computer and an Ettus Research B200mini universal software radio peripheral (USRP) to cre-

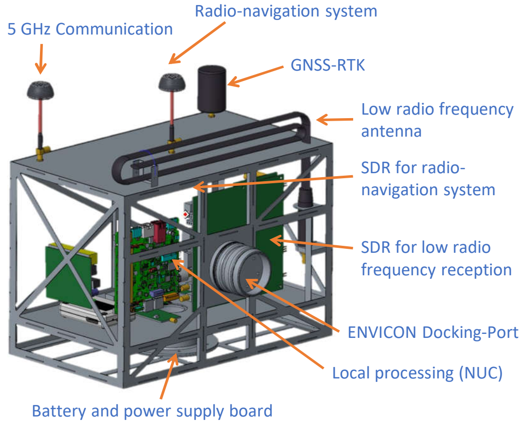

Figure 4: Concept of one LOFAR payload box with major internal components shown.

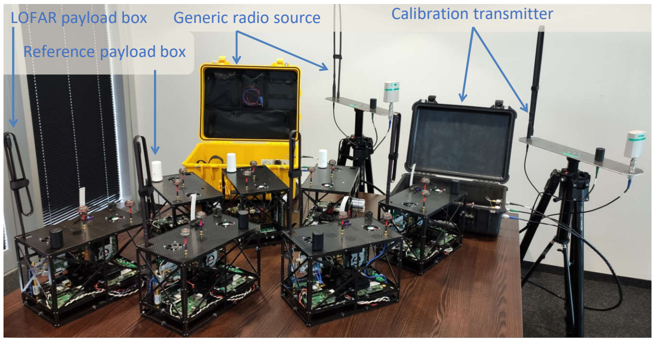

Figure 5: All seven payload boxes integrated before dust protective cover is applied. Two low radio frequency transmitters are built, which can be manually deployed in the field.

ate a software-defined radio (SDR). We process the physical layer, medium access control layer, and the localization system in real-time on the Intel NUC, see Sec. 5. The low radio frequency signal receiver is also integrated as SDR and consists of the same Intel NUC, but an additional Ettus Research N200 USRP, low noise amplifier (LNA), and an unfolding whip-antenna. For power supply, we make use of a small integrated battery and the developed PBIMS.

In addition to the four LOFAR payload boxes, we realized three payload boxes without the low radio frequency components. Those three payload boxes support the antenna localization based on the radio-localization system, see Sec. 5, and we refer to them as reference boxes throughout this paper. Fig. 5 shows all seven payload boxes after integration without the protective dust cover and optical markers. Two low radio frequency transmitters have been built additionally, which serve as a calibration transmitter and a generic radio source. Their usage is described in the proof of concept array operation in Sec. 6.

4. AUTONOMOUS ROBOTIC ARRAY DEPLOYMENT

Mission Control of Heterogeneous Robotic Team

To orchestrate our team of robotic agents, the high-level mission control software *ROSMC* was used [12]. The framework allows for straightforward mission specification and monitoring due to its user-friendly graphical interfaces. From the control room, it communicates with the robots about the tasks to be executed to achieve the mission goal, i.e., to complete the deployment of the payload boxes. A set of the highest-level skills of our robotic agents is exposed to the operators. They can compose a mission with sequentially combined skills, each of which can be intuitively parameterized via interactive markers in a 3D visualization. *ROSMC* also receives status reports from the robots, such as high-level updates on their activities as well as the latest results of the visual mapping process, which are all critical to the successful and efficient mission operation and in-situ adaptation.

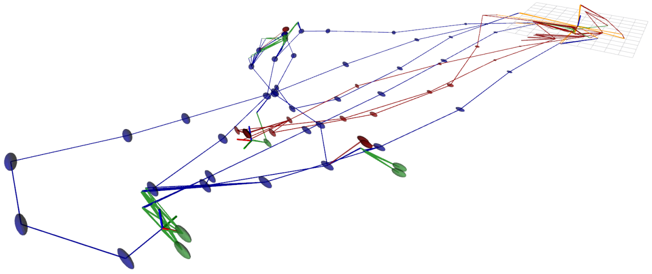

Figure 6: Visualization of the SLAM graph for the multi-robot team during the stacking of a LOFAR payload box over the respective power payload box. Blue and red ellipsoids correspond to the origins of submaps from the two rovers, LRU1 and LRU2, respectively. Green ellipsoids correspond to the positions of each deployed payload box. Yellow lines correspond to inter-robot detections, which happened mostly when revisiting the lander site.

Multi-Robot Mapping and Autonomous Navigation

A critical component for the coordination of our team of robotic agents, operating in semi-autonomy for the deployment of LOFAR payload boxes, is our distributed multi-robot simultaneous localization and mapping (SLAM) system. Described in detail in [13], [14], it allows to create accurate maps of the environment following repeated detections of terrain features [15], but also known objects, i.e., deployed payload boxes and robots belonging to the team. At its core, the SLAM system optimizes over time a graph of poses, associated to *submaps*, which are local representations of the environment, as well as robot and object locations. An optimization step follows the establishment of inter-pose constraints, which are constructed with the help of detecting *AprilTags*, visual markers mounted on the robots, the lander, and payload boxes. Apart from the purpose of mapping, our SLAM system is therefore fundamental to correct the estimation of the deployment location of each payload box. This limits the positioning error associated to the deployment of the following boxes to the pose estimation drift of the last traverse starting from the lander location, instead of the one accumulated from the beginning of the entire mission. It also allows for a compensation of estimation errors within the deployment area of the LOFAR array when sequentially observing multiple payload boxes, thereby improving the relative localization estimates of the payload boxes w. r. t. each other.

Fig. 6 shows a snapshot of the SLAM graph during the demonstration mission, corresponding to the moment where LRU2 stacked a LOFAR payload box over the power payload box that was placed beforehand. While LRU2 was instructed

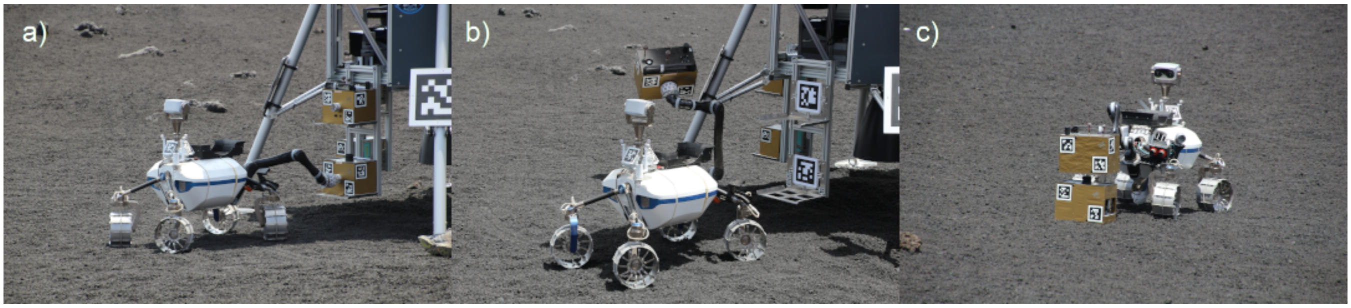

Figure 7: Images of the LRU2 rover manipulating the payload boxes during the construction of one element of the LOFAR array: The LRU2 rover picks the power payload box (a) and the LOFAR payload box (b) at the lander and couples the payload boxes in the field (c).

to traverse the slope between the lander and the deployment location for the first stack, LRU1 visited the places where all the deployed boxes were located, enforcing additional constraints in the SLAM graph towards a more accurate estimation of their position with respect to each other and to the lander.

Mobile manipulation of LOFAR infrastructure

The LRU2 rover can autonomously deploy the power and LOFAR payload boxes in the field, when requested by mission control. The main architecture and components necessary to perform these operations were developed for a previous set of experiments, where the rover deployed an array of seismic instruments at the same experiment site [16].

The architecture is centered around a *world model*, which the rover adapts while observing the environment. The world model is an internal representation of the robot's knowledge about the current real-world situation. Within the robot, it centrally manages the heterogeneous aspects of the real world, such as physical geometries as well as virtual approaches, grasps, and storages. A tree structure is employed, where nodes represent objects while links represent homogeneous transformations. This representation allows for specifying complex physical relations among objects in a highly-abstracted manner by utilizing parent-child relationship. The world model has specific interfaces to each of the following individual components necessary for the autonomous deployment:

The state-machine execution software RAFCON orchestrates the other components by querying services to either observe or interact with the environment [17]. The hierarchical state-machine design allows for intuitive programming of complex behaviors, and online monitoring of the current execution state. During the mission, the operator can connect to the state machine execution, visualize the current state, and manually control the flow if necessary.

The object detector software for the payload boxes and lander is based on a hierarchical composition of tags, which are integrated into the payload box design. The tag-based detection approach with multiple redundant tags provides robust visual localization of the prior known objects under outdoor conditions and optimizes the detected pose with the information gained by detecting multiple tags in one camera image.

The motion planning software computes collision-free motions for the integrated six-degree-of-freedom manipulator, based on the current geometric state of the internal world model. The algorithm searches the space of joint motions for a currently feasible motion, based on the observations of the environment. Fig. 8 shows the computed approach motion when deploying the LOFAR payload box on the power payload box during the experiment.

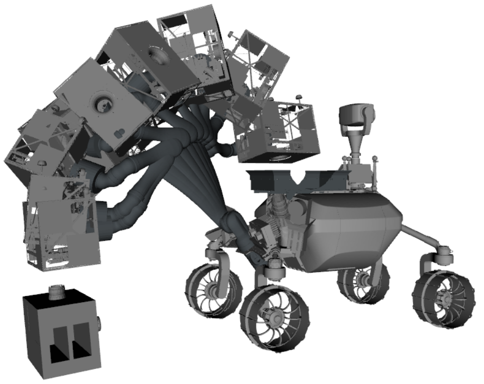

Figure 8: Visualization of the planned approach motion to place and couple the LOFAR payload box on top of the power payload box, computed on-board the LRU2 rover.

Figure 9: Images from the lander camera during the autonomous deployment of the power payload box (top) as well as the LOFAR payload box (bottom) with the LRU2 rover.

The impedance controller of the manipulator enables the rovers to actively control the forces of the end-effector during the infrastructure deployment [18]. The software senses

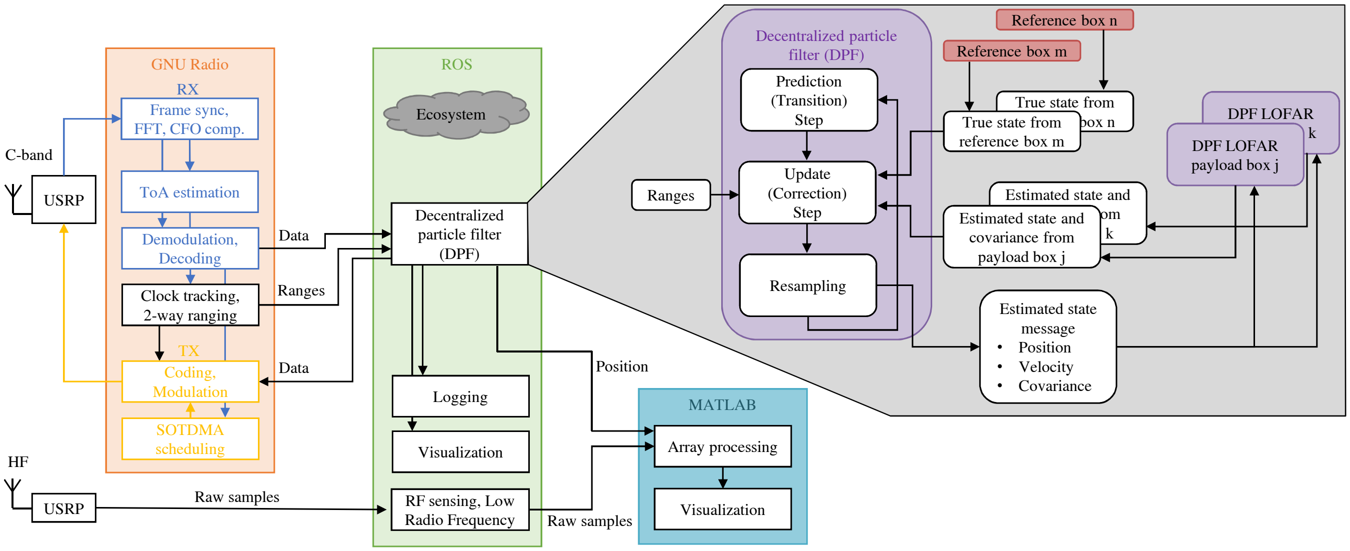

Figure 10: Radio-localization system tailored to the ARCHES LOFAR mission based on the swarm-navigation ecosystem developed at DLR.

the currently enacted forces on the end-effector or attached instrument, based on the measured joint torques. The controller creates a virtual spring between the current pose and the desired pose of the end-effector. The programmer can intuitively parameterize the spring with a desired stiffness to create the desired contact behavior.

The ENVICON docking interface at the end-effector of the manipulator allows to couple different tools and instruments, and allows the rover to establish a defined and rigid connection to the individual objects. To counter the uncertainties of the manipulation process, introduced by the object detection as well as the modelling errors in the manipulator, the docking interface allows for a tolerance of approximately $2\,\mathrm{cm}$ based on the design of the mechanism.

Equipped with these capabilities, the LRU2 rover was able to autonomously complete one part of the ARCHES LOFAR array during the demonstration mission. First, the rover detected the lander with the object detector and drove to the payload box shelf, where the manipulator grasped the power payload box and stored the box in the rover payload compartment, as shown in Fig. 7 (a). After driving to the deployment location, the manipulator deposited the power payload box in the field, see the top part of Fig. 9. Second, the rover fetched the LOFAR payload box from the lander, see Fig. 7 (b), and stacked it onto the power payload box in the field - securing the power supply of the LOFAR payload box, see the bottom part of Fig. 9 and Fig. 7 (c).

To stack the payload boxes, the rover detected the power payload box with the object detector to re-localize the relative position. The manipulator docked the LOFAR payload box with the docking interface and the motion planner computed a safe approach motion from the transport compartment as show in Fig. 8. During the contact, the impedance controller controlled the forces between the two payload boxes and the rover successfully docked the two payload boxes.

5. RADIO-LOCALIZATION SYSTEM FOR ARRAY LOCALIZATION

The payload boxes are placed by the rover LRU2 based on the visual navigation system, as described in the previous sections. At mission design, it has been clear from the beginning that visual navigation localization uncertainties of the boxes, approximated to be between $5\,\%$ to $10\,\%$ of the traveled distance, must be taken into account. In general, the antenna positions of a phased array, be it distributed or centralized, must be known accurately w. r. t. the operation wavelength, which is $15\,\mathrm{m}$ for our proof of concept array operation at $20\,\mathrm{MHz}$ carrier frequency. DLR develops a so-called swarm-navigation system, which is a wireless radio system jointly enabling communication, localization, and timing for networked robots and sensors [19], [20]. From this swarm-navigation system, we used the localization component, tailored it for the ARCHES LOFAR mission, and refer to it as radio-localization system throughout this paper.

Our radio-localization concept is based on estimating the round-trip time of flight of radio signals exchanged between our radio nodes, and on decentralized estimation algorithms to obtain an accurate position estimate of each LOFAR payload box. We refer to this round-trip time of flight estimation as ranging. Our approach makes use of all LOFAR payload boxes and reference boxes operating as a meshed network in a cooperative fashion. Additionally, we integrated the radio-localization system into the lander to obtain a network of in total eight radio nodes for localization. The height difference between the antenna of the radio-localization system mounted on the lander and the LOFAR payload boxes was about $6\,\mathrm{m}$. Due to this geometry, we were able to demonstrate and use 2D, 2.5D, and 3D localization. Finally, we used the 3D position estimates from the radio-localization system as input for the array operation.

Fig. 10 provides an overview of the radio-localization system tailored to the ARCHES LOFAR mission [20]. The integrated USRP enables us to receive and transmit radio signals defined in the complex baseband. Signal bandwidth and carrier frequency can flexibly be chosen. We use the open-source framework GNU Radio, where we realized the physical layer

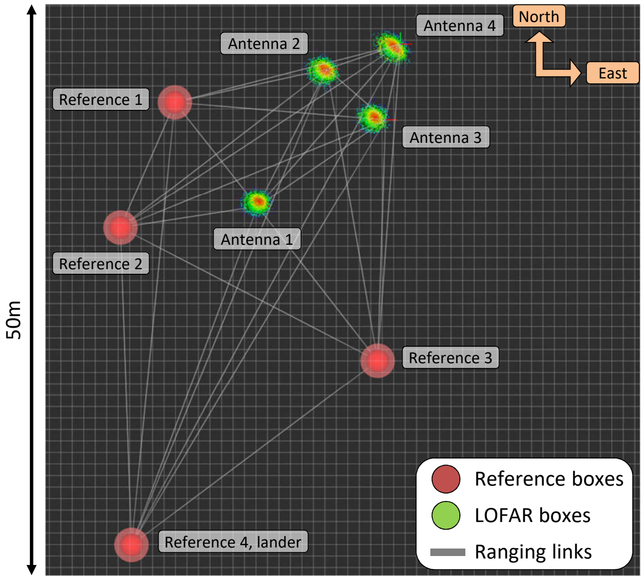

Figure 11: Snapshot of the operator's GUI with visualized position estimates of all four LOFAR payload boxes. Ranging links in grey show current connectivity and hence, availability of raw observations for our cooperative localization approach.

and medium access control layer processing for ranging. The decentralized particle filter used to estimate the relative position of each LOFAR payload box uses the middleware Robot Operating System (ROS) for data exchange. With this approach, we enable simplified interfacing in the robotics domain. Each LOFAR payload box contains one distributed particle filter (DPF). The DPF exchange their estimated state, such as position, together with the corresponding covariance with the DPFs of the neighboring LOFAR payload boxes. After few iterations within this network, the estimated positions can be obtained and used as input for array processing in Sec. 6. We also developed a graphical user interface (GUI), which attaches to our ROS interfaces, such that an operator in the control room can observe the current system state.

The result of the LOFAR payload box localization based on the radio-localization system is shown in Fig. 11. The array is about 50 m away from the lander, and for better comparability, we transformed the estimated LOFAR payload box positions into the local GNSS-RTK east north up (ENU) frame. The whole network consisting of reference boxes, lander, and LOFAR payload boxes is well connected, resulting in good position estimates of all four antennas of the array. During the final demonstration day on Mt. Etna, one reference box failed and was not operational anymore. Yet, we were able to successfully estimate the positions of all four antennas, which demonstrates the robustness of our decentralized, cooperative approach for self-localization. We experienced a small degradation in the localization accuracy, in particular for antenna number four, but we were still able to operate the array as intended with minor signal direction of arrival estimation and beamforming performance degradation.

6. PROOF OF CONCEPT ARRAY OPERATION

In the following subsections, we describe the array operation in detail: the array geometry and configuration, setup, calibration and operation modes, as well as final results of signal direction-of-arrival (DoA) estimation and beamforming.

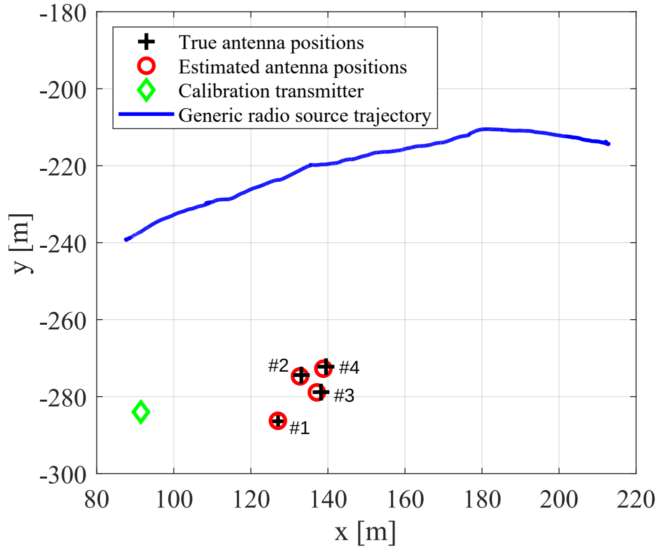

Figure 12: Track of the generic radio source carried across the experiment area. The starting point has been on the left.

Array Geometry

The design of the array geometry is driven by the following aspects and constraints. The maximum number of LOFAR payload boxes is limited to four. This limit is set by the available resources in the project and the planned overall duration for deployment and operation in the analog campaign on Mt. Etna. We also need to take properties of the phased array, such as good direction-of-arrival (DoA) estimation performance and minimized grating lobes, as well as properties of self-localization from the radio-localization system into account. For example, to estimate DoA well along the broadside of an array, one would setup a uniform linear array with half wavelength separation. However, this geometry is sub-optimal for self-localization, as ranging links perpendicular to the linear array are missing and thus not constraining the self-localization error in this direction. As a result, we define the array geometry in a diamond-shape: antennas number two, three, and four form a equidistant triangle of one half of the wavelength. Antenna number one is separated by one wavelength to improve DoA estimation in one direction. In order to account for any misplacement during robotic deployment, we scale the initial array geometry to 90 %. This down-scaling reduces the precision of DoA estimation, but we gain robustness for this minor precision reduction by allowing a larger margin of positioning error: If due to self-localization errors, the robot would deploy antennas number two, three, four with more than one half of the wavelength separation, we would obtain unwanted grating lobes and thus, unwanted ambiguities for DoA estimation.

Modes of Operation and Setup

In general, phased arrays enable two operational modes. The first operation mode is the estimation of the DoA in azimuth or elevation of a radio source. A second operation mode is beamforming, e.g., pointing the main lobe of the array to a certain direction to improve the signal to noise ratio (SNR). Another beamforming use case is steering the array such that an interfering radio signal is placed into a spatial null. In our analog campaign, we demonstrated all these use cases: DoA estimation, and beamforming for SNR improvement as well as spatial nulling.

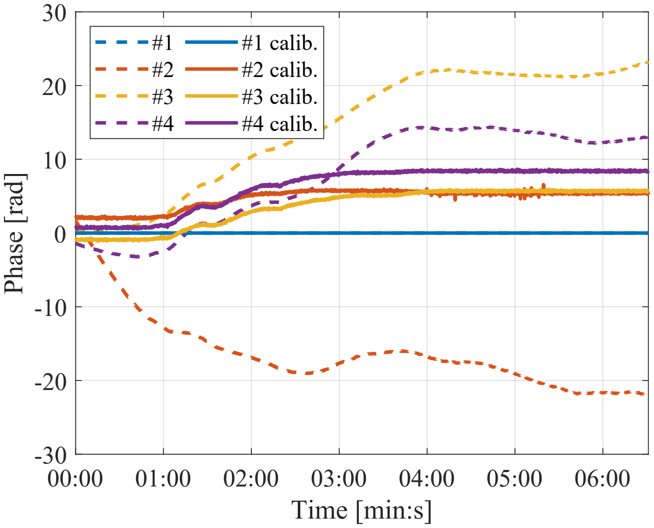

Figure 13: Low radio frequency signal phase evolution of the generic radio source. Dashed lines show the uncalibrated phases and solid lines calibrated phases based on the calibration transmitter. At time spans $0\,\mathrm{min}$ - $1\,\mathrm{min}$ and $4\,\mathrm{min}$ - $6\,\mathrm{min}$ the generic radio source has been kept static. The phase drift of the uncalibrated system is visible.

One important aspect for this analog campaign has been the phase calibration of this distributed phased array. For this reason we use a dedicated low radio frequency transmitter with known location relative to the array as calibration transmitter. The calibration transmitter emits a single carrier signal at a carrier frequency of $20\,\mathrm{MHz}$ with an offset of $20\,\mathrm{kHz}$. We use a second transmitter referred to as generic radio source, which emits a single carrier signal at a carrier frequency of $20\,\mathrm{MHz}$ with an offset of $100\,\mathrm{kHz}$. The position of the generic radio source is unknown to the array, and serves as a signal source to be estimated for the two operation modes.

DoA Estimation Result

For proof of concept DoA estimation we use the generic radio source mounted on a tripod and carry it across the experiment area, see Fig. 12. In our analog-campaign, we focus on the azimuth only. The trajectory is chosen such that we cover the broadside of the array, where DoA estimation should work well, as well as the end-fire side of the array, where DoA estimation becomes challenging. At the beginning of the trajectory and at the end, we kept the tripod static to observe the measured phase evolution.

Fig. 13 shows the phase evolution measured with the array. Phases are related to antenna number 1, hence the phase evolution for this element is zero. We clearly see a significant phase drift at time spans where the generic radio source on the tripod has been kept static. This phase drift is caused by the internal oscillator of each SDR in each LOFAR payload box. To compensate for that, we jointly estimate the calibration parameters and azimuth DoA. Solid lines in Fig. 13 show the phase evolution after applying the estimated calibration parameters for compensation. Whenever the generic radio source is not moving, the phase evolution should remain constant: see time spans $0\,\mathrm{min}$ - $1\,\mathrm{min}$ and $4\,\mathrm{min}$ - $6\,\mathrm{min}$ in Fig. 13.

The estimated azimuth DoA and its ground-truth are shown in Fig. 14. We obtain ground-truth DoA by using a GNSS-RTK receiver integrated in the generic radio source equipment. We can clearly see a very good match between the estimated azimuth DoA and the ground-truth, with some differences at the end of the trajectory, which is the end-fire side of the array. To get a better qualitative view of the azimuth DoA estimation error, we show the absolute error in Fig. 15. Throughout the trajectory until we reach the end-fire side, we obtain an absolute error below 3° and partially even sub-degree accuracy. This is a very good result given that we calibrated the array with only one specific DoA, as the calibration transmitter has always been at the same position. Commonly, one would calibrate the array for multiple DoAs distributed over the manifold. Additionally, estimated antenna positions resulting from our radio-localization system are not error-free.

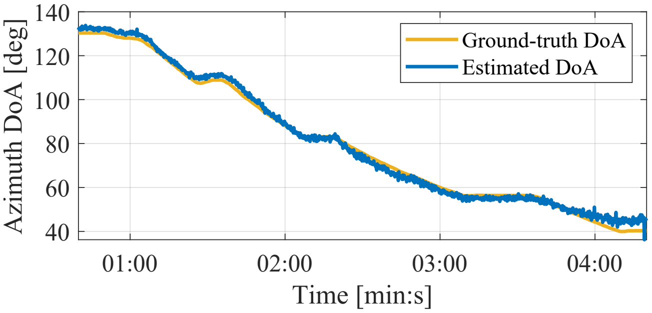

Figure 14: Estimated azimuth DoA and corresponding ground-truth along the trajectory depicted in Fig. 12. We can observe a very good match between the estimate and ground-truth with an increased error at the end-fire side of the array.

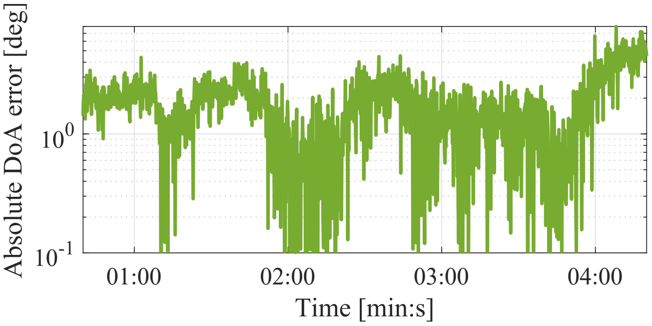

Figure 15: Absolute azimuth DoA estimation error along the trajectory. The y-axis is log-scaled to better see the estimation error ranging from few degrees to sub-degrees.

Beamforming Result

The beamforming mode follows the same concept as for DoA estimation w.r.t. array calibration. In this mode, we specifically steer the array such that, e.g., the antenna gain maximum points to a desired direction. Received signals at each antenna can then be coherently combined in baseband with the estimated array calibration parameters and the defined steering vector. We demonstrated this on Mt. Etna, and we present two examples in this paper. Both examples have been demonstrated live, and in real-time based on the observed signal from the generic radio source.

The first example consists of focusing the array in the direction of the generic radio source, where we assume the direction to the source as known. The left polar plot in Fig. 16 shows the resulting antenna pattern. We coherently combine

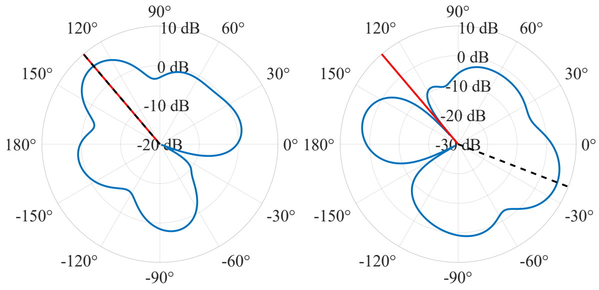

Figure 16: Resulting antenna gain pattern for two beamforming examples. The red line indicates the signal direction of the generic radio source, and the black dashed line the set focusing direction. The left plot shows the beam focused into the direction of the generic radio source. The right plot shows the spatial nulling of the generic radio source.

the received signals from all four antennas, and the result is shown in the upper plot of Fig. 17. The increased power of the resulting coherently combined signal at 100 kHz offset from the 20 MHz carrier frequency is visible. Having a closer look at the received signal power at all four antennas, we can determine a loss of the total combining gain of 0.4 dB.

The second example consists of spatially nulling the generic radio source. To achieve this, we steered the array based on the array calibration parameters to determine the spatial null. The right plot in Fig. 16 shows the resulting antenna pattern. In our case, we can spatially null the generic radio source by focusing the array to about $-20°$. We coherently combine the received signals from all four antennas, and observe a significantly reduced total signal power in the lower plot in Fig. 17.

Single Antenna Performance

As mentioned in Sec. 3 we had to balance weight, functionality, and overall resources for this proof of concept demonstration. In general, our used unfolding whip antenna is electrically very short, and we took this into account for the array operation. Antennas with appropriate length realized as, e.g., unrolling self-stabilized tube-like structure are available but were out of scope for this demonstration.

7. DISCUSSION ON DEVELOPED TECHNOLOGIES

In general, our developed technologies for the ARCHES LOFAR mission presented in this paper can be used for any planetary surface exploration. Our modular payload carrier concept can be used as a base design to develop scientific instrument packages in a standardized fashion. The developed robotic capabilities, ranging from autonomous navigation in unstructured environments to manipulation, enable multi-robot exploration. The swarm-navigation system, from which we only use the localization component in this analog-campaign, enables joint communication, navigation, and timing for networks of robots and sensors [21] for exploration on the surface, as well as in caves and lava tubes. This system in particular can be fused with visual navigation, and a potential future lunar satellite based communication and navigation system. Additionally, we can make use of the collaborative nature of networked robots and sensors, to allow for joint calibration and control [22], [23].

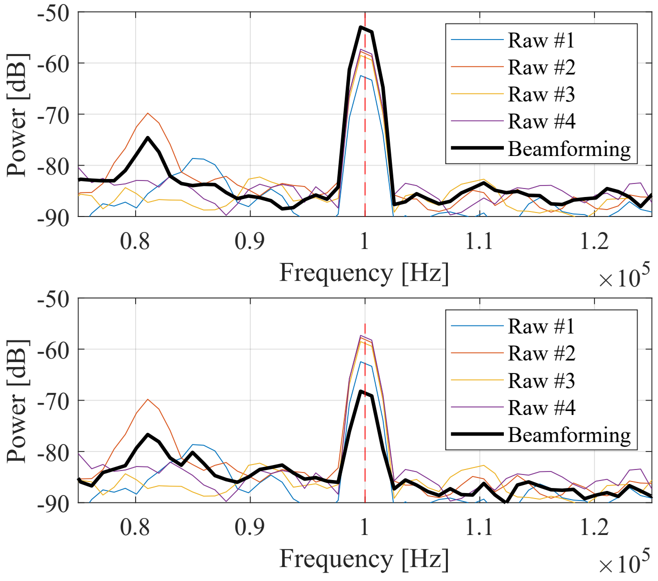

Figure 17: Signal spectrum after coherent signal combination based on the array steering vector. The upper plot shows the case when focusing the beam into the direction of the generic radio source, where as the lower plot shows the result for the spatial nulling case. The generic radio source emits a signal at 100 kHz offset from the 20 MHz carrier frequency.

8. SUMMARY

In this work, we describe our developed technologies to enable distributed low radio frequency arrays to establish a radio telescope on the lunar far side. Our technologies include modular payload carriers, autonomous robotic array deployment, and cooperative radio-localization to accurately determine the array geometry. We selected an experiment site on the volcano Mt. Etna, Sicily, Italy, to test, and demonstrate our technologies in an analog campaign over the course of four weeks in June and July 2022. The ARCHES LOFAR mission has been a full success. We were able to demonstrate all steps of the mission resulting in a proof of concept operation demonstration of the low radio frequency array.

ACKNOWLEDGMENTS

Part of the presented research has been supported by the Helmholtz Association project ARCHES (contract number ZT-0033), and the DLR projects Planetary Exploration and Swarm-Navigation. We would also like to thank Bernard Foing, who is now with the University of Leiden, Netherlands and has been with European Space Agency (ESA) when the ARCHES project started, for his scientific advice. Additionally, we have to thank all our numerous students and colleagues not mentioned in the author list who contributed to this mission and its success.

REFERENCES

[1] J. O. Burns, G. Hallinan, J. Lux, L. Teitelbaum, J. Kocz, R. MacDowall, R. Bradley, D. Rapetti, W. Wu, S. Furlanetto, A. Austin, A. Romero-Wolf, T.-C. Chang, J. Bowman, J. Kasper, M. Anderson, Z. Zhen, J. Pober, and J. Mirocha, "NASA probe study report: Farside array for radio science investigations of the dark ages

and exoplanets (farside)," 2019. [Online]. Available: https://arxiv.org/abs/1911.08649

[2] L. V. E. Koopmans, R. Barkana, M. Bentum, G. Bernardi, A.-J. Boonstra, J. Bowman, J. Burns, X. Chen, A. Datta, H. Falcke, A. Fialkov, B. Gehlot, L. Gurvits, V. Jelić, M. Klein-Wolt, J. Lazio, D. Meerburg, G. Mellema, F. Mertens, A. Mesinger, A. Offringa, J. Pritchard, B. Semelin, R. Subrahmanyan, J. Silk, C. Trott, H. Vedantham, L. Verde, S. Zaroubi, and P. Zarka, "Peering into the dark (ages) with low-frequency space interferometers," *Experimental Astronomy*, vol. 51, no. 3, pp. 1641 – 1676, 2021.

[3] European Space Agency, "ESA strategy for science at the moon," pp. 1 –49, May 2019. [Online]. Available: https://exploration.esa.int/web/moon/-/61371-esa-strategy-for-science-at-the-moon

[4] van Haarlem, M. P. *et al.*, "LOFAR: The LOw-Frequency ARray," *Astronomy & Astrophysics*, vol. 556, p. A2, 2013. [Online]. Available: https://doi.org/10.1051/0004-6361/201220873

[5] P. McGarey, I. A. Nesnas, A. Rajguru, M. Bezkrovny, V. Jamnejad, J. Lux, E. Sunada, L. Teitelbaum, A. Miller, S. W. Squyres, G. Hallinan, A. Hegedus, and J. O. Burns, "How to deploy a 10-km interferometric radio telescope on the moon with just four tethered robots," in *2022 IEEE Aerospace Conference (AERO)*, 2022, pp. 1 – 8.

[6] S. Bandyopadhyay, J. Lazio, A. Stoica, P. Goldsmith, B. Blair, M. Quadrelli, J.-P. de la Croix, and A. Rahmani, "Conceptual ideas for radio telescope on the far side of the moon," in *2018 IEEE Aerospace Conference (AERO)*, 2018, pp. 1 – 10.

[7] A. Wedler *et al.*, "Finally! insights into the arches lunar planetary exploration analogue campaign on etna in summer 2022," in *Proceedings of the International Astronautical Congress (IAC)*. International Astronautical Federation, 2022.

[8] M. J. Schuster *et al.*, "Towards Autonomous Planetary Exploration: The Lightweight Rover Unit (LRU), its Success in the SpaceBotCamp Challenge, and Beyond," *Journal of Intelligent & Robotic Systems (JINT)*, Nov. 2017. [Online]. Available: https://doi.org/10.1007/s10846-017-0680-9

[9] A. F. Prince, B. Vodermayer, B. Pleintinger, A. Kolb, E. Staudinger, E. Dietz, S. Schröder, S. Frohmann, F. Seel, and A. Wedler, "Design and implementation of a modular mechatronics infrastructure for robotic planetary exploration assets," in *Proceedings of the International Astronautical Congress (IAC)*. International Astronautical Federation, 2021.

[10] A. Wedler *et al.*, "First Results of the ROBEX Analogue Mission Campaign: Robotic Deployment of Seismic Networks for Future Lunar Missions," in *Proc. of the Int. Astronautical Congr., IAC*, vol. 68. Adelaide, Australia: Int. Astronautical Federation (IAF), Sep. 2017.

[11] A. F. Prince, B. Vodermayer, B. Pleintinger, A. Kolb, G. Franchini, E. Staudinger, E. Dietz, S. Schröder, S. Frohmann, F. Seel, and A. Wedler, "Modular mechatronics infrastructure for robotic planetary exploration assets in a field operation scenario," in *Proceedings of the International Astronautical Congress (IAC)*. International Astronautical Federation, 2022.

[12] M. J. Schuster *et al.*, "The ARCHES Space-Analogue Demonstration Mission: Towards Heterogeneous Teams of Autonomous Robots for Collaborative Scientific Sampling in Planetary Exploration," *IEEE Robotics and Automation Letters (RA-L)*, vol. 5, no. 4, pp. 5315–5322, Oct 2020.

[13] M. J. Schuster, K. Schmid, C. Brand, and M. Beetz, "Distributed stereo vision-based 6d localization and mapping for multi-robot teams," *Journal of Field Robotics*, vol. 36, no. 2, pp. 305–332, 2019.

[14] M. J. Schuster, "Collaborative Localization and Mapping for Autonomous Planetary Exploration: Distributed Stereo Vision-Based 6D SLAM in GNSS-Denied Environments," Ph.D. dissertation, University of Bremen, 2019. [Online]. Available: http://nbn-resolving.de/urn:nbn:de:gbv:46-00107650-19

[15] R. Giubilato, M. Vayugundla, W. Stürzl, M. J. Schuster, A. Wedler, and R. Triebel, "Multi-modal loop closing in unstructured planetary environments with visually enriched submaps," in *2021 IEEE/RSJ International Conference on Intelligent Robots and Systems (IROS)*. IEEE, 2021.

[16] P. Lehner, S. Brunner, A. Dömel, H. Gmeiner, S. Riedel, B. Vodermayer, and A. Wedler, "Mobile manipulation for planetary exploration," in *2018 IEEE Aerospace Conference*. IEEE, 2018, pp. 1–11.

[17] S. G. Brunner, F. Steinmetz, R. Belder, and A. Dömel, "Rafcon: A graphical tool for engineering complex, robotic tasks," in *2016 IEEE/RSJ International Conference on Intelligent Robots and Systems (IROS)*. IEEE, 2016, pp. 3283–3290.

[18] A. Albu-Schäffer, C. Ott, and G. Hirzinger, "A unified passivity-based control framework for position, torque and impedance control of flexible joint robots," *The international journal of robotics research*, vol. 26, no. 1, pp. 23–39, 2007.

[19] E. Staudinger, S. Zhang, R. Poehlmann, and A. Dammann, "The role of time in a robotic swarm: A joint view on communications, localization, and sensing," *IEEE Commun. Mag.*, vol. 59, no. 2, pp. 98–104, 2021.

[20] S. Zhang, R. Pöhlmann, E. Staudinger, and A. Dammann, "Assembling a swarm navigation system: Communication, localization, sensing and control," in *2021 IEEE 18th Annual Consumer Communications Networking Conference (CCNC)*, 2021, pp. 1–9.

[21] S. Zhang, K. Cokona, R. Pöhlmann, E. Staudinger, T. Wiedemann, and A. Dammann, "Cooperative pose estimation in a robotic swarm: Framework, simulation and experimental results," in *Proc. 30th European Signal Processing Conf. (EUSIPCO)*, Belgrad, Serbia, 2022.

[22] R. Pöhlmann, E. Staudinger, S. Zhang, and A. Dammann, "Simultaneous localization and calibration for radio navigation on the moon: Results from an analogue mission," in *ION GNSS+ 2022*, September 2022. [Online]. Available: https://elib.dlr.de/188065/

[23] R. Pöhlmann, S. Zhang, E. Staudinger, A. Dammann, and P. A. Hoeher, "Simultaneous localization and calibration for cooperative radio navigation," *IEEE Trans. Wireless Commun.*, vol. 21, no. 8, pp. 6195–6210, 2022.

BIOGRAPHY

***Emanuel Staudinger** received the M.Sc. degree in Embedded Systems Design from the University of Applied Sciences of Hagenberg, Austria, in 2010. Since 2010, he is with the Institute of Communications and Navigation of the German Aerospace Center (DLR), Wessling, Germany. He received a Ph.D. with distinction from the Institute of Electrodynamics and Microelectronics at the University of Bremen, Germany, in 2015. His current research interests include system design for cooperative positioning, experimental platform design based on SDRs, and experimental validation for swarm navigation. Within ARCHES he was responsible for the LOFAR mission design, and related system development for the radio-localization system, as well as proof of concept array operation.*

***Robert Pöhlmann** received the B.Sc. and the M.Sc. degrees in Electrical Engineering and Information Technology from the Technical University of Munich (TUM) in 2014 and 2016, respectively. In 2013 he joined the Institute of Communications and Navigation of the German Aerospace Center (DLR) as a student trainee and in 2016 he became a research staff member. His current research interests are in the area of statistical signal processing for multi-antenna systems and cooperative localization.*

***Siwei Zhang** received his B.Sc. in electrical engineering from Zhejiang University, China, in 2009, his M.Sc. in communication engineering from the Technical University of Munich, Germany, in 2011, and his Dr.-Ing. (Ph.D.) in electrical engineering from the University of Kiel, Germany, in 2020. In 2012, he joined the Institute of Communications and Navigation of the German Aerospace Center (DLR) as a research staff member. His research interests lie in statistical signal processing in wireless communication and navigation, particularly in multi-agent joint communication, navigation and sensing. He is a recipient of the 2021 DLR Science Award.*

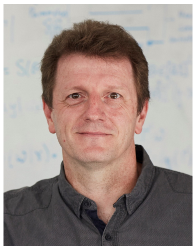

***Armin Dammann** received the Dipl.-Ing. (M.Sc.) and Dr.-Ing. (Ph.D.) degrees in Electrical Engineering from the University of Ulm, Germany, in 1997 and 2005 respectively. In 1997 he joined the Institute of Communications and Navigation of the German Aerospace Center (DLR) as a research staff member. Since 2005 he is head of the Mobile Radio Transmission Research Group. His research interest and activities include signal design and signal processing for terrestrial wireless communication and navigation systems. In these fields, he has been active in several EU-projects, e.g., WINNER, WHERE and WHERE2. Armin Dammann is lecturer at the Technical University of Munich for* Robot and Swarm Navigation.

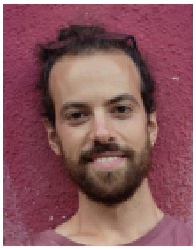

***Riccardo Giubilato** received the Ph.D. degree in Space Sciences, Technologies and Measurements in 2020 from the Centre of Studies and Activities for Space (CISAS) "G. Colombo," University of Padova. Since 2019, he is Post-Doctoral researcher with the German Aerospace Center (DLR), Institute of Robotics and Mechatronics, Weßling, Germany. His current research interests include multi-robot SLAM, sensor fusion for vision systems and range sensors, multimodal and learning-based place recognition in unstructured environments.*

***Ryo Sakagami** is a researcher at the Department of Cognitive Robotics at the Institute of Robotics and Mechatronics, German Aerospace Center (DLR) since 2020. His research focus is on the world model for autonomous, intelligent robotic systems, especially with mobile manipulation capabilities. He received his master's degree in engineering from the University of Tokyo in 2020.*

***Peter Lehner** is a researcher at the Institute of Robotics and Mechatronics, German Aerospace Center (DLR), since 2014. He received his master's degree in Computer Engineering from the Technical University of Berlin in 2014. Currently he leads the team on robotic mobile manipulation and his research activities include developing methods for autonomous motion generation for mobile manipulation systems to empower mobile robots to autonomously interact with their environment.*

***Martin J. Schuster** is a senior researcher and leader of the Planetary Exploration Operations team at the Institute of Robotics and Mechatronics of DLR. He received his Ph.D. (Dr.-Ing.) degree in Computer Science (CS) from the University of Bremen in 2019, his first Master's degree in CS from the Georgia Institute of Technology in Atlanta, USA in 2010, his Bachelor's and second Master's degree in CS from the Technische Universität München (TUM) in 2008 and 2011, and his Bachelor's degree in Philosophy from the Ludwig-Maximilians-Universität München (LMU) in 2014. His research focus is on multi-robot SLAM in GNSS-denied areas.*

***Andreas Dömel** is a researcher at the Department of Cognitive Robotics at the Robotics and Mechatronics Center, German Aerospace Center (DLR). He received his Dipl.-Ing. degree in electrical and information engineering in 2010 from the Technical University of Munich. Since 2010 he is with the Institute of Robotics and Mechatronics. His research interests are probabilistic motion planning and design of complex autonomous robotic systems.*

Bernhard Vodermayer *received his degree computer science in 2006 at the Technical University of Munich while he has been scientifically associated with the Institute of Robotics and Mechatronics since 2004. Till 2012, he played a major key role in the development and the technology transfer of the DLR's left ventricular heart assist device DLR-LVAS. Since 2010, he is scientifically related to space based technologies for safe robotic docking and energy management of wheeled, autonomous vehicles for planetary exploration. His research interests are in the field of novel, future emerging technology based actuator and sensor systems, polymer-based systems and related production processes, space technologies, mobile space robotics as well as biomedical devices and active implants. Within ARCHES he is responsible for hardware related system development and coordination of hardware integration and operation.*

Andre F. Prince *received his M.Sc. degree in Mechatronics Engineering from the Politecnico di Torino, Italy in 2020. Since then, he has been working in the Robotics and Mechatronics Institute at the German Aerospace Center (DLR) as Mechatronics engineer. He has contributed to the firmware development in the central electronic box of the Martian Moons Exploration (MMX) rover's locomotion subsystem. Within ARCHES, he has worked on the mechatronics interfaces, hardware and software integration as well as power management and data handling systems. His fields of interest are electronics communication, motor control, and power electronics within robotic planetary exploration.*

Armin Wedler *received his Diploma in Mechanical Engineering and Bachelor in Robotics from Leibniz University of Hanover in 2004 and his PhD in 2010. Starting in 2006, he worked for Leibniz University of Hanover until he joined the Institute of Robotics and Mechatronics, German Aerospace Center (DLR), in 2008. Since then, he has been focusing on the design and development of advanced space robotics, planetary exploration and mobile systems. He has worked as project manager, technical manager and member of project teams for numerous industrial and scientific robotic projects and is coordinator of the DLR groups for mobile robots (since 2015) and for the planetary exploration group (since 2014).*